

Article

Thermal Behavior and Kinetics of Shenmu Coal Pyrolyzed under Hydrogen-Rich or Methane-Gas-Rich Atmosphere

Chong Zou, Xi Li, Mengmeng Ren, Weian Wang and Hao Wu * 

School of Metallurgical Engineering, Xi'an University of Architecture and Technology, Xi'an 710311, China

* Correspondence: whyk20151121@163.com

Abstract: The pyrolysis characteristics of Shenmu coal under an atmosphere containing H₂ (40%) and another containing CH₄ (40%) were studied via a thermogravimetric analysis, and the kinetic parameters of pyrolysis were calculated by using a distributed activation energy model (DAEM). The results showed that H₂ promoted the cleavage of CH-like functional groups by providing reactive hydrogen groups to combine with CH groups and –OH groups in the coal. However, the H₂ and CH₄ atmosphere inhibits the cleavage of oxygen-containing functional groups such as carbonyl groups and C–O groups, and this is unfavorable to the production of CO₂ and CO. The pyrolysis weight-loss rate of raw coal decreases with the increase of the heating rate, and the weight-loss curve shifts to the high-temperature region. At the same conversion rate and pyrolysis temperature, the activation energy of pyrolysis under the H₂ and CH₄ atmospheres is lower than that under the N₂ atmosphere, and the activation energy does not conform to the Gaussian distribution. The activation energy of pyrolysis was distributed in a narrow range, in which the activation energy of the H₂ and CH₄ atmospheres was concentrated in the range of 175–215 kJ/mol and 225–230 kJ/mol, respectively, and the activation energy of the H₂ atmosphere was lower than that of the CH₄ atmosphere under the same conversion rate.

Keywords: thermogravimetric analysis; pyrolytic atmosphere; pyrolytic properties; distributed activation energy model (DAEM); activation energy



Citation: Zou, C.; Li, X.; Ren, M.; Wang, W.; Wu, H. Thermal Behavior and Kinetics of Shenmu Coal Pyrolyzed under Hydrogen-Rich or Methane-Gas-Rich Atmosphere. *Energies* **2023**, *16*, 2339. <https://doi.org/10.3390/en16052339>

Academic Editor: Javier Feroso

Received: 1 February 2023

Revised: 12 February 2023

Accepted: 24 February 2023

Published: 28 February 2023



Copyright: © 2023 by the authors. Licensee MDPI, Basel, Switzerland. This article is an open access article distributed under the terms and conditions of the Creative Commons Attribution (CC BY) license (<https://creativecommons.org/licenses/by/4.0/>).

1. Introduction

The Shenfu–Dongsheng coalfield is one of the large coalfields in the world, with an area of about 11,000 km² and proven coal reserves of 230 billion tons. The raw coal produced in the coal field has the characteristics of low ash, low sulfur, low phosphorus, and high volatile [1], especially its high oil content (about 10%), which is very suitable for extracting tar from coal by medium- and low-temperature pyrolysis [2–4]. At present, the actual annual processing of low-grade coal through the pyrolysis process in this area has exceeded 60 million tons. Commonly used pyrolysis reactors include a moving bed, fluidized bed, and rotary furnace. The pyrolysis conditions of different reactors include the temperature [5], pressure [6], heating rate [7], and atmosphere [8]. The first three influencing factors have been deeply studied, and the influence of pyrolysis atmosphere has attracted the attention of researchers in recent years due to the fact that H₂, CH₄, and other gases generally exist in the atmosphere of the pyrolysis reactor, and the content may be high. These gases can participate in the stabilization of free radicals and the reconstruction of chemical bonds in coal, resulting in the differences of pyrolysis characteristics and products. Zhang et al. [9] investigated the effects of different atmospheres on coal pyrolysis by using a small fluidized bed. The results show that a H₂ atmosphere will reduce the yield of semi-coke and increase the yield of tar. A CH₄ atmosphere will increase the yield of semi-coke at 800 °C and promote an increase in the tar yield at a high temperature. In addition, a reducing atmosphere is conducive to the light weight of tar. Zhong et al. [10] studied the effects of different reaction atmospheres on the distribution and composition

of coal pyrolysis products at a pyrolysis temperature of 850 °C in a fluidized bed. The results showed that the addition of H₂ at a faster heating rate reduces the yield of tar, while CH₄ promotes the formation of tar. A CH₄ atmosphere can promote the formation of alkyl naphthalene and benzene, and its split carbon can increase the yield of semi-coke. Fidalgo et al. [11] studied the effect of syngas (H₂/CO) on the yield of tar from coal pyrolysis by using a fixed bed reactor. At the same time, the properties of tar were characterized by gas chromatography, mass spectrometry, and infrared spectroscopy. Compared with N₂, syngas (H₂/CO) can obtain a higher pyrolysis tar yield and lighter tar. In addition, the tar obtained from syngas (H₂/CO) has greater aromaticity and is rich in oxygen-containing functional groups. Jin et al. [12] studied the effects of different atmospheres on the yield and properties of coal pyrolysis products in a fixed bed reactor. The results showed that H₂ reduced the yield of semi-coke by inhibiting the secondary reaction in the pyrolysis process, H₂ and CO₂ promoted the yield of H₂O through the reverse reaction of water gas reaction, while CO inhibited the reaction, and CH₄ promoted the content of benzene and phenols in tar; CO can also inhibit the formation of phenols. It can be seen that researchers pay more attention to the effect of pyrolysis atmosphere on the yield of dry distillation products and the properties of tar.

In addition, the diversity of coal structure also leads to the complexity of coal pyrolysis behavior. Therefore, there are many models describing coal pyrolysis process, mainly including a single reaction model [13], total package reaction model [14], distributed activation energy model (DAEM) [15], and Friedman differential model and Ozawa Flynn wall analysis method [16], and the kinetic parameters obtained by different methods will also be different.

The DAEM method was first proposed by Vand [17] to describe the resistance-change behavior of metal films and then applied by Pitt [18] to the field of coal pyrolysis. It is considered that the infinite parallel reaction model can be used to describe the infinite parallel reaction in the process of coal pyrolysis. After long-term development, Miura et al. [19] finally proposed a new distributed activation energy model, the Miura integral method. This method does not need to make assumptions about the activation energy distribution and pre-exponential factor in advance. The activation energy and pre-exponential factor can be obtained directly by integral method through experimental data, that is, DAEM method has good adaptability to complex coal pyrolysis reaction. It can accurately describe the pyrolysis process of coal in a wide pyrolysis temperature range, and its model is consistent with the pyrolysis process of coal, so it has been widely used [20]. Alonso et al. [21] found that the apparent activation energy of coal pyrolysis process proceeds with the increase of conversion, and the distribution of activation energy is different in the pyrolysis process of different coal grades. Zhang et al. [22] established a new parallel reaction model based on the distributed activation energy model and then obtained the pyrolysis reaction kinetic model parameters. Using the model, the pyrolysis behavior of two low-rank coals was predicted, and the practicability of the model was verified by experiments. The results showed that the model has a wide application range. Li et al. [23] analyzed the pyrolysis kinetic characteristics of Lignite by using the DAEM method. The results showed that the activation energy of coal pyrolysis process increases with the increase of weight loss rate, but for the distribution function of the pyrolysis process $f(E\alpha)$, the curve is not Gaussian. Zhao et al. [24] studied the applicability of DAEM method in their study of the overall kinetics of the coal pyrolysis process and analyzed the influence of weight loss in water loss and degassing and secondary degassing stages of coal pyrolysis on the results of the DAEM method. The results showed that the activation energy distribution function of the coal-pyrolysis process obtained by the DAEM method had good independence in water loss and degassing and secondary degassing weight loss stages, and it is reliable in a wide pyrolysis temperature range. Wang et al. [25] conducted basic research on the pyrolysis characteristics of coal by combining experimental and modeling methods and obtained the kinetic parameters by using the DAEM method. The results show that the distributed activation energy model can effectively describe the main characteristics of

coal pyrolysis process. To sum up, because the DAEM method does not involve a complex pyrolysis reaction mechanism, it can accurately describe the pyrolysis process of coal in a wide pyrolysis temperature range. There are few studies on the influence of pyrolysis atmosphere on coal pyrolysis kinetics, among which H₂ and CH₄ atmospheres have less influence on the calculation results of the DAEM method [26,27].

In this research, a thermogravimetric analysis was used to study the effect of pyrolysis atmosphere containing H₂ and CH₄ on the pyrolysis characteristics of low-order coal. In this paper, the conversion of functional groups during pyrolysis, the distribution characteristics of gas products under different pyrolysis atmospheres, and the behavior of pyrolysis under different pyrolysis heating rates are discussed. The kinetic parameters of coal pyrolysis in a pyrolysis atmosphere containing H₂ and CH₄ were calculated by using a distributed activation energy model (DAEM), and the influencing reasons and differences of coal pyrolysis kinetics in pyrolysis atmosphere containing H₂ and CH₄ were analyzed. We expect to provide basic data for the study of pyrolysis atmosphere as an influencing factor in the process of coal pyrolysis.

2. Experiment

2.1. Materials

The coal samples used in the experiment were Shenmu low-rank coal. The results of proximate and ultimate analysis are shown in Table 1. The coal samples with particle size less than 75 µm were vacuum-dried at 100 °C for 4 h and stored in sealed bags. Their proximate analysis and ultimate analysis are shown in Table 1. Semi-coke samples were prepared by holding coal samples at 450 °C, 550 °C, 650 °C, and 750 °C for 30 min in a tubular furnace. The carrier gases of the pyrolysis reaction were N₂ (99.999%), H₂ (60%N₂, 40%H₂), and CH₄ (60%N₂, 40%CH₄), respectively. The carrier gas flow rate was 50 mL/min, and the carrier gas was injected through the hole at the bottom of the reactor. The semi-coke samples were cooled in a N₂ atmosphere and then sealed in sample bags.

Table 1. Proximate analysis and ultimate analysis of coal samples.

| Rank Coal | Proximate Analysis/% | | | | Ultimate Analysis/% | | | | |
|--------------|----------------------|-----------------|------------------|------------------|---------------------|------------------|-------------------|------------------|------------------|
| | M _{ad} | A _{ad} | V _{daf} | FC _{ad} | C _{daf} | H _{daf} | O* _{daf} | N _{daf} | S _{daf} |
| | 3.83 | 7.53 | 37.06 | 55.97 | 71.97 | 4.38 | 22.51 | 0.93 | 0.2 |

ad, air-drying base; daf, dry-ash-free base; *, difference method.

2.2. TG-MS Analysis

The pyrolysis characteristics of raw coal were studied by using SETARAMSETSIS thermogravimetric analyzer (France) and Pfeiffer quadrupole mass spectrometer (TG-MS) (Germany). Thermogravimetric and mass spectrometer were connected through quartz capillary (heated to 200 °C to avoid the condensation of gas generated by pyrolysis of thermogravimetric analyzer). The change of sample weight was recorded by the thermal analysis balance. The gas components generated from pyrolysis were analyzed by suction of a small amount of gas [H₂ (*m/z* = 2), CH₄ (*m/z* = 16), H₂O (*m/z* = 18), CO (*m/z* = 28), CO₂ (*m/z* = 44)] in the ion chamber of mass spectrometer through capillary, and the change of gas with the increase of pyrolysis temperature was recorded online in real time. In each case, the mass of pulverized coal was 10 mg, the reaction carrier gas was N₂ (99.999%), H₂ atmosphere (60%N₂, 40%H₂), and CH₄ atmosphere (60%N₂, 40%CH₄), and the flow rate was 50 mL/min. The programmed heating rates were 5 °C/min, 7.5 °C/min, 10 °C/min, 15 °C/min, from room temperature to 850 °C, and the experiment was carried out under atmospheric pressure.

2.3. FTIR Analysis

Functional group information of coal samples was provided by FTIR spectroscopy (FTIR, Nicolet IS5, Thermo Fisher Scientific Company, Waltham, MA, USA). The sample

was prepared by using KBr compression, with a scanning range of 400–4000 cm^{-1} and a resolution of 4 cm^{-1} . Figure 1 shows the infrared spectrum of raw coal [28]. It can be seen that low-rank coal is rich in various types of hydroxyl groups (3370 cm^{-1}), and CH functional groups such as $-\text{CH}_3$ (1438 cm^{-1}) and $-\text{CH}_2$ (2925 cm^{-1}) formed by aliphatic and aromatic chains, which can be pyrolyzed into gaseous products such as H_2 , CH_4 , and H_2O .

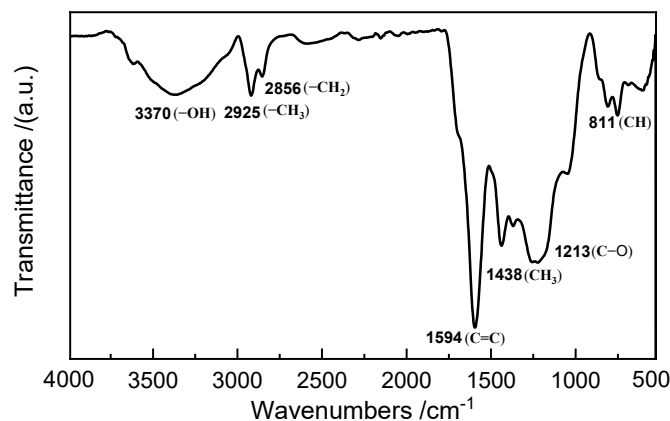


Figure 1. FTIR of raw coal.

2.4. Distributed Activation Energy Model

The distributed activation energy model (DAEM) adopts the assumption of infinite parallel one-stage reactions, which should be well adapted to the solid phase and can describe the reaction process well in a wide range of temperature intervals and ramping rates [29].

The distributed activation energy model (DAEM) is based on two assumptions [30]:

- (1) Infinite parallel reaction hypothesis: The reaction system is composed of numerous independent first-order reactions with different activation energies.
- (2) Activation energy distribution hypothesis: The activation energy of each reaction presents a continuous distribution and conforms to a certain functional form.

The weight-loss rate at any time (t) in the pyrolysis weight-loss process is given by the following Equation (1):

$$\frac{w}{w_0} = 1 - \int_0^\infty \exp\left(-k \int_0^t \exp\left(-\frac{E_\alpha}{RT}\right) dt\right) f(E_\alpha) dE_\alpha \quad (1)$$

where w is the sample weight loss at any time, t ; w_0 is the initial sample weight; k_0 is the pre-exponential factor corresponding to activation energy E_α ; T is the temperature, $R = 8.314$ is the gas constant; and $f(E_\alpha)$ is the activation energy distribution function, which satisfies Equation (2).

$$\int_0^\infty f(E_\alpha) dE_\alpha = 1 \quad (2)$$

According to the further analysis of the distributed activation energy model (DAEM) by Miura et al. [19], a simplified and accurate method for calculating the activation energy distribution curve $f(E_\alpha)$ and pre-exponential factor (k_0) is the Miura integral method.

$$\ln\left(\frac{h}{T^2}\right) = \ln\left(\frac{k_0 R}{E_\alpha}\right) + 0.6075 - \frac{R}{RT} \quad (3)$$

The activation energy (E_α) is obtained from the above formula, using the pre-exponential factor (k_0) and activation energy distribution function $f(E_\alpha)$. The steps are as follows:

- (1) At least three weight loss curves under different heating rates were obtained.
- (2) According to the selected weight loss curve, the same conversion α makes the $\ln(h/T^2)-1/T$ curve correspond to the temperature data.
- (3) A series of Arrhenius straight lines with the same conversion can be obtained by making different heating rates on the $\ln(h/T^2)-1/T$ diagram. The activation energy, $E\alpha$, at different conversion can be calculated from the slope of these straight lines.
- (4) With α to $E\alpha$, the distribution activation energy function $f(E\alpha)$ is obtained via the differential calculation of the obtained curve.

For the activation energy ($E\alpha$) and activation energy distribution function $f(E\alpha)$ in the calculation process, the change of volatile matter is taken as the starting point. Since the pyrolysis process of low-order coal will cause dehydration, degassing, thermal decomposition, and thermal condensation, in turn, when calculating the pyrolysis kinetics, it is necessary to eliminate the interference of water on the kinetic calculation and select 150 °C as the initial temperature for pyrolysis volatilization analysis.

3. Results and Discussion

3.1. Thermogravimetric Analysis

Figure 2 shows the pyrolysis weight-loss curves of raw coal under N₂, H₂ (40%), and CH₄ (40%) atmospheres (pyrolysis heating rate of 15 °C/min). As can be seen from Figure 2a, with the increase of pyrolysis temperature, compared with the N₂ atmosphere, the pyrolysis TG curve of coal moves to the low-temperature zone in the H₂ (40%) and CH₄ (40%) atmospheres; that is, the H₂ and CH₄ atmospheres promote the pyrolysis weight loss of coal. According to the DTG curve in Figure 2b, the coal pyrolysis process can be divided into three stages. The first stage is from room temperature to about 380 °C, which is the gas adsorbed by the removal of external and part of internal water, coal gap CO₂, and hydrocarbon organic small molecules in the initial stage of coal pyrolysis. The second stage is about 380–550 °C, mainly depolymerization and decomposition reaction, which is the most important stage of coal pyrolysis weight loss. In the third stage, the secondary thermal polycondensation of coal occurs, and H₂ is mainly precipitated. It can be seen from Table 2 that, among the three stages of coal pyrolysis, in the first stage, H₂ and CH₄ atmospheres have no significant effect on the weight loss of coal pyrolysis. In the second stage, the pyrolysis weight loss of coal in the H₂ atmosphere was significantly higher than that in the N₂ atmosphere (22.96 and 18.38%), and the pyrolysis weight loss in the CH₄ atmosphere (19.57%) was also greater than that in the N₂ atmosphere; in the third stage, the pyrolysis weight loss in the H₂ and CH₄ atmosphere (8.65 and 7.13%, respectively) was less than that in the N₂ atmosphere (10.09%). In addition, the fastest pyrolysis weight-loss rate in the H₂ and CH₄ atmosphere (0.179%/°C and 0.147%/°C) was higher than that in N₂ atmosphere (0.134%/°C). It can be seen that the atmospheres containing H₂ and CH₄ have little effect on the weight loss of coal pyrolysis at a lower pyrolysis temperature. At a higher pyrolysis temperature, the atmosphere containing H₂ and CH₄ can promote the pyrolysis of coal, and the promotion effect of the H₂ atmosphere is more obvious. The analysis shows that the activity of the H₂ molecule or hydrogen radical will increase with the increase of the pyrolysis temperature. The cracking of organic macromolecules and the fracture of functional groups in coal will produce small molecular groups, which are easy to combine with active hydrogen to form stable small molecular compounds, thus promoting the release of volatiles. In addition, it can be seen from Figure 2b that the pyrolysis temperature exceeds about 750 °C; the TG curve in the CH₄ atmosphere shows obvious weight gain, which may be due to the partial carbon reaction [31] in CH₄ atmosphere at high temperature; and the generated carbon particles are adsorbed to the surface of the crucible, resulting in the reduction of weight loss.

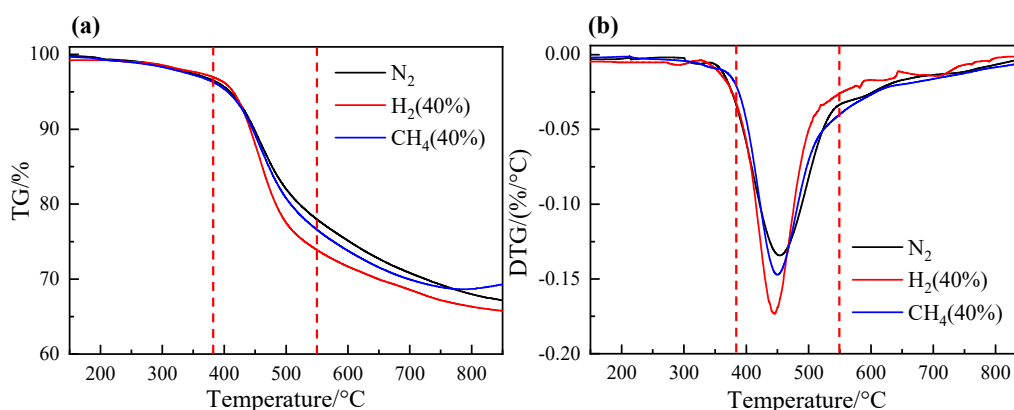


Figure 2. TG–DTG curves of coal pyrolysis under different heating rates in N₂, H₂ (40%), and CH₄ (40%): (a) TG curves and; (b) DTG curves.

Table 2. Pyrolysis characteristics of different pyrolysis stages.

| Atmosphere | Total Weight Loss/% | Weight Loss I/% | Weight Loss II/% | Weight Loss III/% | $(d_w/d_t)_{max}$ (%/°C) |
|-----------------------|---------------------|-----------------|------------------|-------------------|--------------------------|
| N ₂ | 32.23 | 3.76 | 18.38 | 10.09 | 0.134 |
| H ₂ (40%) | 34.86 | 3.25 | 22.96 | 8.65 | 0.179 |
| CH ₄ (40%) | 30.68 | 3.98 | 19.57 | 7.13 | 0.147 |

3.2. Gas Product Release Analysis

In Figure 3, the release curves of H₂, CH₄, H₂O, CO, and CO₂ during coal pyrolysis in N₂, H₂ (40%), and CH₄ (40%) atmospheres are shown, respectively. It can be seen from Figure 3a that the release range of CH₄ gas during coal pyrolysis is mainly focused on the second and third stages of thermal weight loss. The release sources of CH₄ gas mainly include the shedding of various functional groups in raw coal and the decomposition reaction of methyl and methoxy functional groups in the fat chain or aromatic chain. In addition, in the middle and later stage of pyrolysis, methyl or methylene functional groups react with free H• to produce CH₄ [10].



It can be seen from the reaction that the release of CH₄ is closely related to methyl and free hydrogen. It can be seen from Figure 3a that the release intensity of CH₄ gas during coal pyrolysis in the H₂ atmosphere is higher than that in the CH₄ and N₂ pyrolysis atmospheres. Figure 4 shows the infrared spectra of semi-cokes prepared in N₂, H₂-containing, and CH₄-containing atmospheres at different pyrolysis temperatures. At the same pyrolysis temperature, the aromatic CH group deformation vibration peak (860–880 cm⁻¹) of semi-coke (H₂ and CH₄) is weaker than that of semi-coke (N₂), while the benzene ring C–H stretching vibration peak (3000–3100 cm⁻¹), the Cycloalkane, or aliphatic hydrocarbon CH₂/CH₃ stretching vibration peak (2920–2950 cm⁻¹) is slightly weaker than semi-coke (N₂). This shows that, under the pyrolysis atmospheres containing H₂ and CH₄, more CH, CH₂, and CH₃ groups are generated during coal pyrolysis; that is, H₂ and CH₄ atmospheres can promote the cracking of aromatic CH groups and aliphatic CH₂ or CH₃ groups in coal, increase free radicals such as CH₃• and CH₂• produced during pyrolysis, and improve the release of CH₄; in the H₂ atmosphere, the promoting effect of is more obvious.

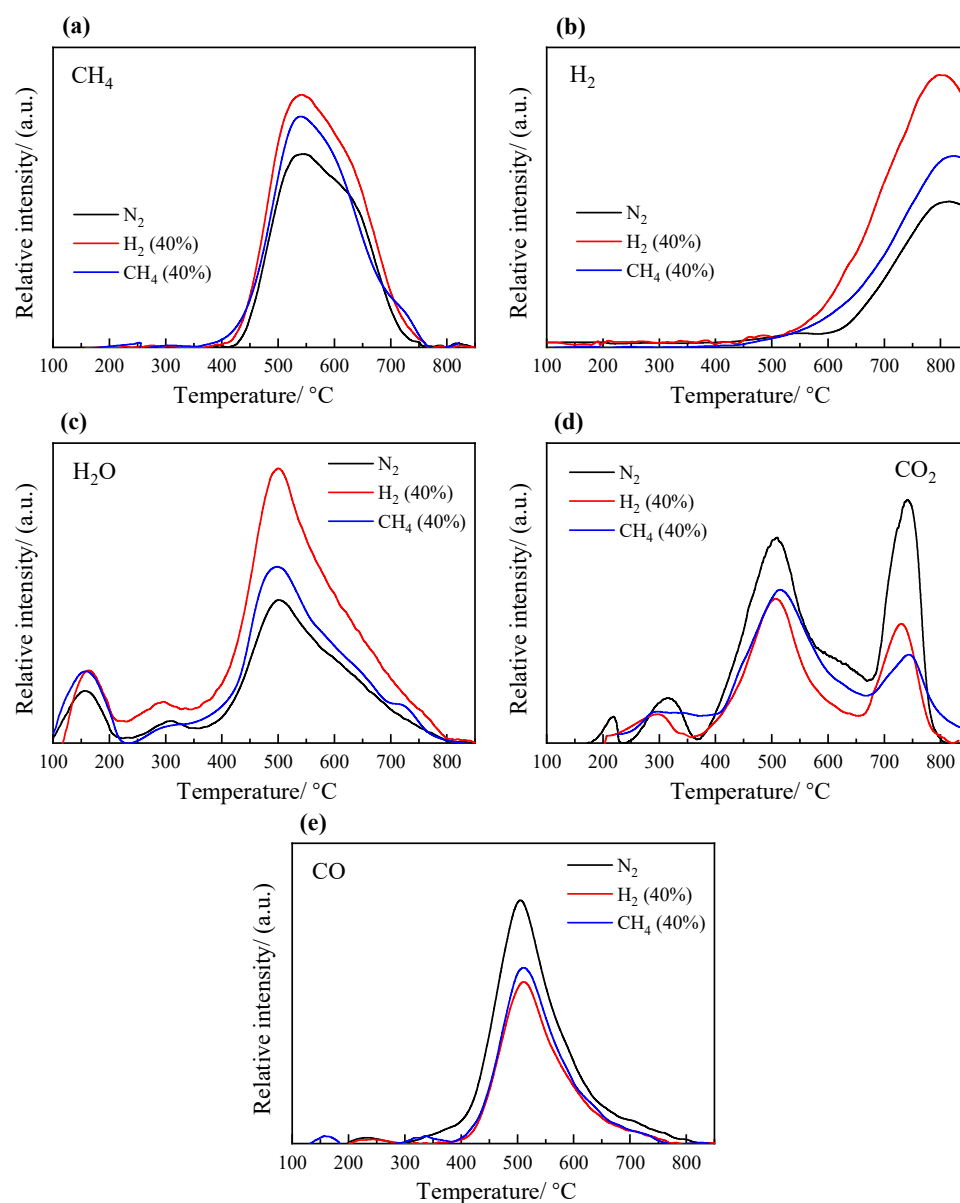


Figure 3. Emission curves of CH_4 , H_2 , H_2O , CO , and CO_2 during coal pyrolysis in N_2 , H_2 (40%), and CH_4 (40%): (a) CH_4 release curve; (b) H_2 release curve; (c) H_2O release curve; (d) CO_2 release curve and; (e) CO release curve.

As can be seen from Figure 3b, there is basically no H_2 release in the first stage of coal pyrolysis. In the second stage, the escape of H_2 comes from the decomposition of some hydrogen-rich matrix in the coal. The main release stage of H_2 is the third stage of pyrolysis, which mainly comes from the condensation reaction of organic matter in coal and the aromatization of hydrocarbons [32]. It can be seen from Figure 4 that, at a higher pyrolysis temperature, the deformation vibration absorption peak of aromatic CH group in the wave number range of $860\text{--}880\text{ cm}^{-1}$ and the benzene ring C–H stretching vibration peak [33] in the wave number range of $3000\text{--}3100\text{ cm}^{-1}$ of semi-coke (H_2 and CH_4) are weaker than that of semi-coke (N_2), in which the deformation vibration absorption peak intensity of C–H group of semi-coke (N_2) is weaker, indicating that H_2 promotes the release of H_2 during coal pyrolysis more than the CH_4 atmosphere does.

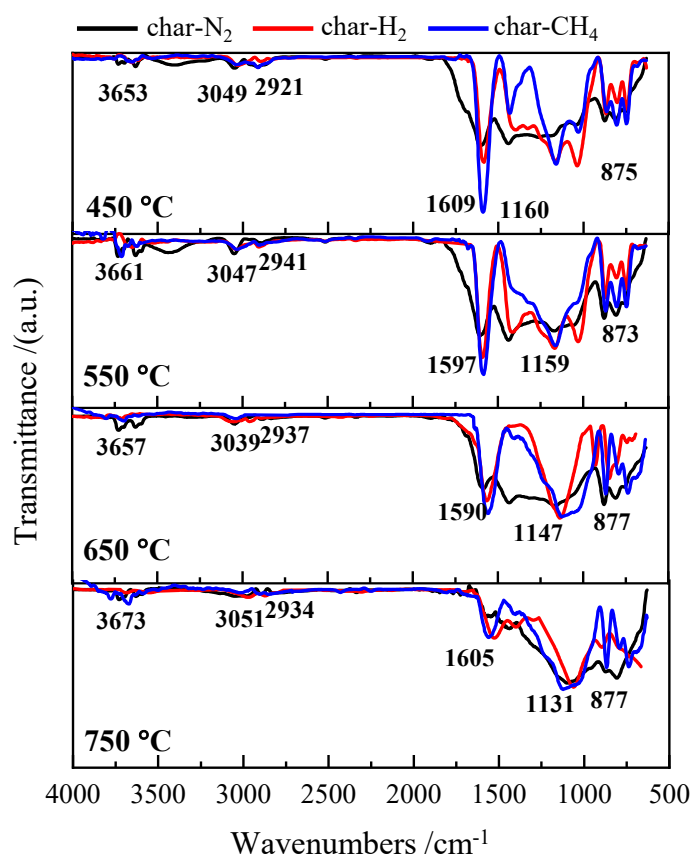


Figure 4. Infrared spectra of semi-coke (N_2 , H_2 , and CH_4) at different pyrolysis temperatures.

Figure 3c is the release curve of H_2O during coal pyrolysis. It can be seen that the release of H_2O is mainly in two temperature ranges. In the first stage of pyrolysis ($100\sim 300\text{ }^\circ\text{C}$), it is mainly the internal and external water and crystalline water in coal. It can be seen that, in the first stage of pyrolysis, the atmospheres containing H_2 and CH_4 have little effect on the release of internal water and crystalline water in coal, and the intensity of the second release peak of H_2O is significantly improved. The second release range of H_2O is mainly the second and third stages of coal pyrolysis; it mainly comes from the decomposition and fracture of various oxygen-containing functional groups (mainly OH groups) in coal and the redox reaction between pyrolysis carrier gases [34]. It can be seen from Figure 4 that, in the second and third stages of pyrolysis, at the same pyrolysis temperature, the absorption peak of semi-coke prepared from the H_2 -containing pyrolysis atmosphere in the wave number range of $3350\sim 3700\text{ cm}^{-1}$ is weaker than that of semi-coke (N_2), the functional groups corresponding to the absorption peak in this wave number range are mainly alcohol/phenol OH stretching vibration and free and associated $-OH$ [35], and the OH absorption peak of semi-coke (H_2) in this wave number range is weaker than that of semi-coke (N_2). This shows that the pyrolysis atmosphere containing H_2 promotes the cracking and release of $-OH$ groups during coal pyrolysis. According to the analysis in Figure 3c, H_2 promotes the combination of active hydrogen groups and $-OH$ to release more H_2O , while the absorption peak intensities of $-OH$ functional groups of semi-coke (CH_4) and semi-coke (N_2) are similar, so it has little effect on the formation of H_2O .

As shown in Figure 3d, there are CO_2 release peaks in the three weight-loss stages of coal pyrolysis. The first release interval is mainly the CO_2 molecules adsorbed on the coal surface and in the gap, the second release interval is mainly the release of the decomposition and fracture reaction of oxygen-containing functional groups such as carboxyl and carbonyl during coal pyrolysis, and the third release stage mainly comes from the decomposition of carbonate minerals in coal ash and the fracture of partially stable oxygen-containing heterocyclic organic matter [36]. As can be seen from the comparison between Figure 3d,e,

the second release range of CO_2 and the release temperature range of CO during coal pyrolysis (380–550 °C) almost coincide. In this temperature release range, groups such as -COOH , C-O , and C=C in coal decompose and break, some will escape in the form of CO , and the others will combine with free oxygen atoms in coal to form CO_2 molecules. It can be seen from Figure 4 that the intensity of the telescopic vibrational absorption peaks [37] representing carbonyl groups and aromatic C=C near 1600 cm^{-1} for semi-coke (H_2 and CH_4) prepared before the pyrolysis temperature of 750 °C are significantly stronger than that of semi-coke N_2 , while the C-O telescopic vibrational absorption peaks [38] in phenol and alcohol groups (range of $1100\text{--}1300\text{ cm}^{-1}$) are also stronger than that of hemi-coke N_2 ; thus, we can infer that the H_2 - and CH_4 -containing atmospheres might have inhibited the breakup decomposition of carbonyl groups, as well as oxygen-containing functional groups, during coal pyrolysis, thus inhibiting the release of CO_2 and CO in the coal pyrolysis process. Therefore, we can infer that the atmosphere containing H_2 and CH_4 may inhibit the fracture decomposition of carbonyl and oxygen-containing functional groups in the process of coal pyrolysis, thus inhibiting the release of CO_2 and CO in the process of coal pyrolysis.

3.3. Effect of Heating Rate on Coal Pyrolysis Process

The TG-DTG curves of raw coal at different heating rates in N_2 , H_2 -containing, and CH_4 -containing atmospheres are shown in Figure 5. It can be seen that, under the N_2 pyrolysis atmosphere, with the increase of heating rate, the difference between the TG and DTG curves is obvious, the pyrolysis weight loss rate of raw coal decreases, and the TG curve moves to a high temperature. Under pyrolysis atmospheres containing H_2 and CH_4 , the variation law of the TG-DTG curve of raw coal is similar to that of the N_2 pyrolysis atmosphere. It can be seen from the DTG data in Table 3 that the maximum weight-loss rate, $(d_w/d_t)_{\text{max}}$, increases, and the DTG peak shifts to the high-temperature zone. This is because the increase of the heating rate has an impact on pyrolysis. The reaction time experienced by the coal sample is shortened, and the heat-transfer lag delays the pyrolysis reaction to a certain extent. The precipitation of volatile matter needs to be carried out at a higher temperature; that is, the precipitated gas and tar cannot be precipitated from the coal sample in time, and within the same pyrolysis temperature range, the pyrolysis weight-loss rate of raw coal will decrease with the increase of heating rate, and the pyrolysis weight-loss curve will move to the high-temperature zone.

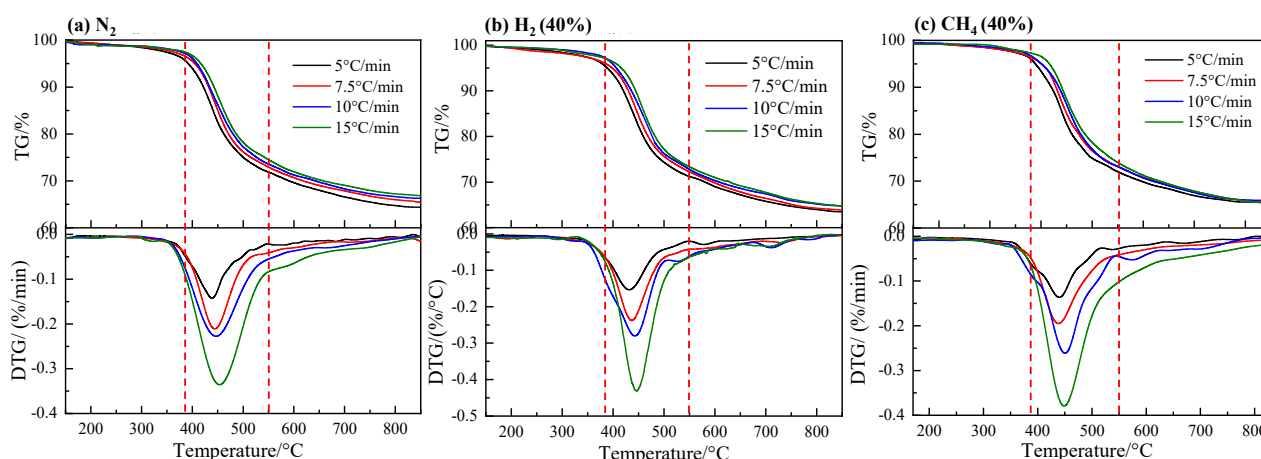


Figure 5. TG–DTG curves of coal pyrolysis: (a) N_2 atmosphere; (b) H_2 (40%) atmosphere and; (c) CH_4 (40%) atmosphere.

Table 3. Pyrolysis characteristic parameters of coal samples at different heating rates.

| Heating Rate/(°C/min) | N ₂ | | H ₂ -40% | | CH ₄ -40% | |
|-----------------------|----------------------|--|----------------------|--|----------------------|--|
| | T _{max} /°C | (d _w /d _t) _{max} %/min | T _{max} /°C | (d _w /d _t) _{max} %/min | T _{max} /°C | (d _w /d _t) _{max} %/min |
| 5.0 | 437.88 | 0.142 | 434.37 | 0.153 | 437.46 | 0.140 |
| 7.5 | 444.87 | 0.211 | 436.70 | 0.237 | 440.15 | 0.209 |
| 10.0 | 447.17 | 0.228 | 442.39 | 0.280 | 446.50 | 0.261 |
| 15.0 | 453.75 | 0.336 | 445.51 | 0.431 | 449.45 | 0.379 |

3.4. Kinetic Analysis

Figure 6 shows the different conversion rates (α) of raw coal in N₂, H₂ (40%), and CH₄ (40%) pyrolysis atmospheres, respectively. The corresponding Arrhenius curve is obtained by selecting a series of data points with conversion rates of 0.1–0.9 from the TG curve to make $\ln(h/T^2)$ and $1/T$ curves, so as to calculate the activation energy ($E\alpha$) at different conversion rates.

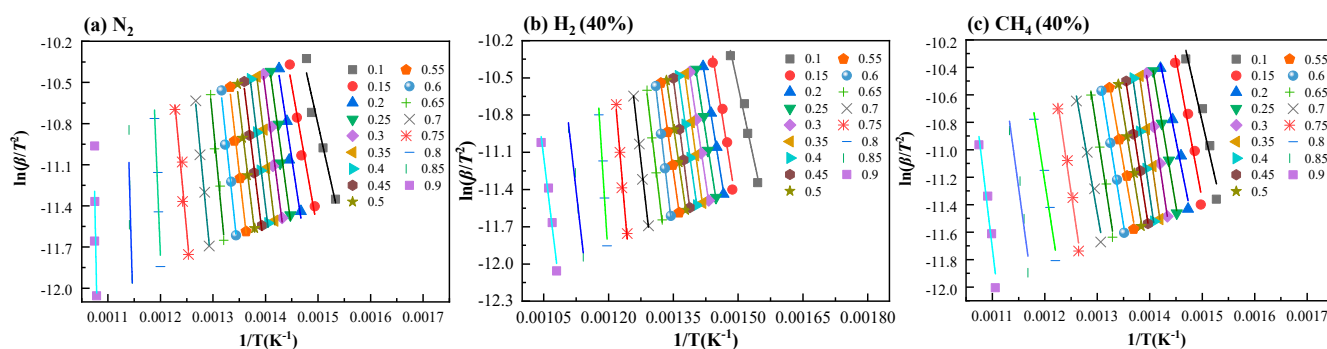


Figure 6. Different conversion α Arrhenius curve of coal: (a) N₂ atmosphere; (b) H₂ (40%) atmosphere and; (c) CH₄ (40%) atmosphere.

It can be seen from Figure 7a that the activation energy, $E\alpha$, of the pyrolysis process shows an increasing trend with the increase of the conversion rate, α , and the pyrolysis temperature under an N₂ atmosphere, H₂ (40%) atmosphere, and CH₄ (40%) pyrolysis atmosphere. At the initial stage of pyrolysis, raw coal is first released in the form of small molecules by the pyrolysis of organic side chains with poor thermal stability and active functional groups, and the required pyrolysis activation energy is small. With the increase of the pyrolysis temperature, the organic chemical bonds in the coal structure continue to break, resulting in tar and a large number of hydrocarbons. The coal structure gradually becomes orderly and increases the difficulty of pyrolysis, so the required pyrolysis activation energy gradually increases. At the same conversion and pyrolysis temperature, the pyrolysis activation energy in the H₂ (40%) and CH₄ (40%) pyrolysis atmospheres is lower than that in the N₂ atmosphere. Among them, the activation energy in the H₂ (40%) atmosphere is slightly higher than that in CH₄(40%) pyrolysis atmosphere, between α 0.1 and 0.2, and lower than that in N₂ atmosphere, in the range from α 0.2 to 0.9. As can be seen from Figure 5b, when α in the range of 0.2–0.7 (interval 0.05), $\ln(\beta/T^2)$ has a good linear correlation with $1/T$, R_2 is above 0.95, and R_2 in the H₂ (40%) atmosphere is slightly higher than that in the N₂ atmosphere and CH₄ (40%) atmosphere. During the initial stage of pyrolysis and thermal condensation, the linear correlation between $\ln(h/T^2)$ and $1/T$ decreased, and its R^2 was in the range of 0.85–0.95. It shows that DAEM method can accurately describe the pyrolysis weight-loss process of low-rank coal in a wide temperature range, and the kinetic parameters obtained are more accurate. As can be seen from Figure 8, compared with the N₂ pyrolysis atmosphere, the distribution of the activation energy of pyrolysis, $E\alpha$, for H₂ (40%) and CH₄ (40%) is very narrow, in which H₂ (40%) is concentrated in the range of 175–215 kJ/mol, while the $E\alpha$ in CH₄ (40%) is concentrated in the range of

225~230 kJ/mol. In addition, the $E\alpha$ in the N_2 pyrolysis atmosphere is mainly distributed in the range of 250~275 kJ/mol. When the conversion exceeds 0.7, $E\alpha$ is distributed in the range of 300~350 kJ/mol.

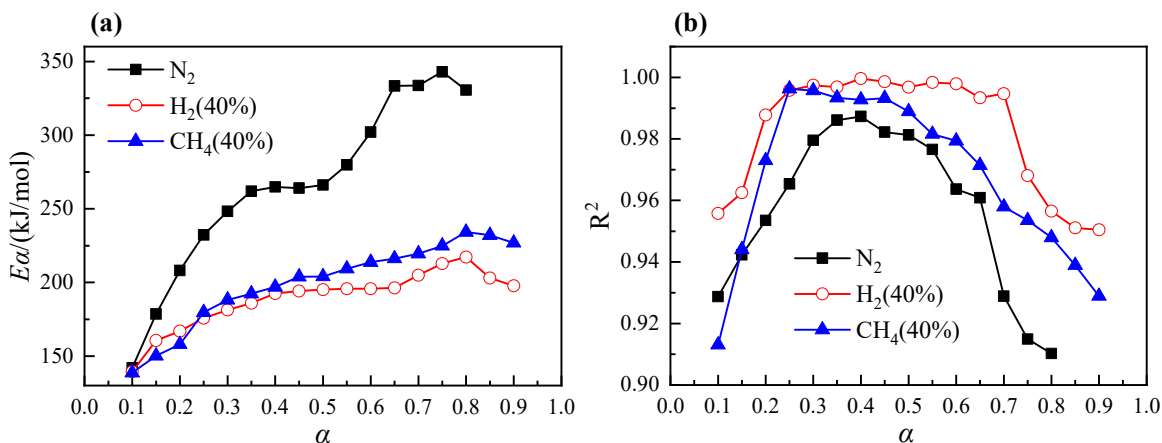


Figure 7. Activation energy, $E\alpha$, and different conversion rates, α , relationship curve: (a) The change curve of $E\alpha$ and; (b) The change curve of R^2 .

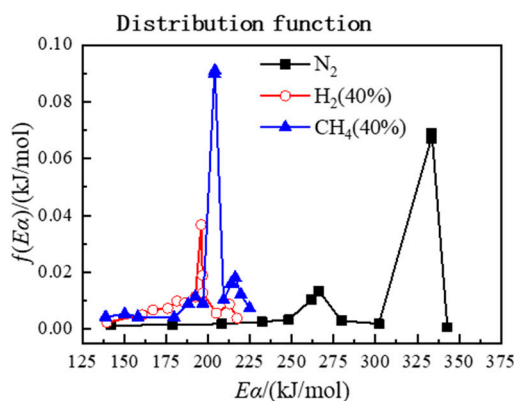


Figure 8. Activation energy, $E\alpha$, distribution density curve.

It is generally considered that the activation energy distribution obtained via the DAEM method conforms to the Gaussian function [39]. that is, the Gaussian distribution can be used to simplify the analysis of coal pyrolysis process. It can be seen from Figure 6 that the activation energy obtained by low-order coal in N_2 , a H_2 (40%) atmosphere, and a CH_4 (40%) pyrolysis atmosphere does not conform to the Gaussian distribution, and this result is consistent with the research results of Miura et al. [19]. It shows that the Gaussian function does not always reflect the true distribution of pyrolysis activation energy. In addition, when the conversion reaches 0.7, the pyrolysis temperature is about 700 °C, most volatile substances in the coal are precipitated, mainly the thermal polycondensation of semi-coke, the decomposition of minerals in ash, and the partial carbon decomposition of CH_4 gas, resulting in the increase of the weight of experimental samples. These factors will lead to a certain impact on the calculation of pyrolysis kinetic parameters by using the DAEM method. In Figure 5b, R^2 is basically above 0.9 in the conversion range of 0.1~0.9, which shows that the DAEM method can accurately describe the pyrolysis process of low-rank coal in a wide temperature range.

In conclusion, at a lower pyrolysis temperature (α about 0.1~0.2), compared with N_2 atmosphere, the H_2 (40%) and CH_4 (40%) atmospheres have less of a promoting effect on coal pyrolysis, the release intensity of the H_2 gas products CH_4 and H_2O is similar to that of the N_2 atmosphere, and the activation energy required for pyrolysis is slightly lower than that for the N_2 atmosphere. With the progress of pyrolysis conversion, the promoting

effect of H₂ (40%) and CH₄ (40%) atmospheres on coal pyrolysis is significantly increased; the release intensity of gas products H₂, CH₄, and H₂O is significantly stronger than that of N₂ atmosphere; and the activation energy required for pyrolysis is also significantly reduced. Compared with CH₄ (40%) atmosphere, the H₂ (40%) atmosphere greatly promotes the pyrolysis of coal. Therefore, under the same conversion rate, the E_α in the H₂ (40%) atmosphere pyrolysis atmosphere is lower than that in the CH₄ (40%) one. Figure 9 shows the schematic diagram of the reaction process; Figure 9a shows the process of H₂ and coal pyrolysis, where H₂ promotes the formation of H₂, CH₄, and H₂O by providing reactive hydrogen groups to combine with CH groups in coal, as well as –OH functional groups, and by promoting the cleavage of CH-like functional groups; and Figure 9b shows the activation energy distribution under the DAEM model.

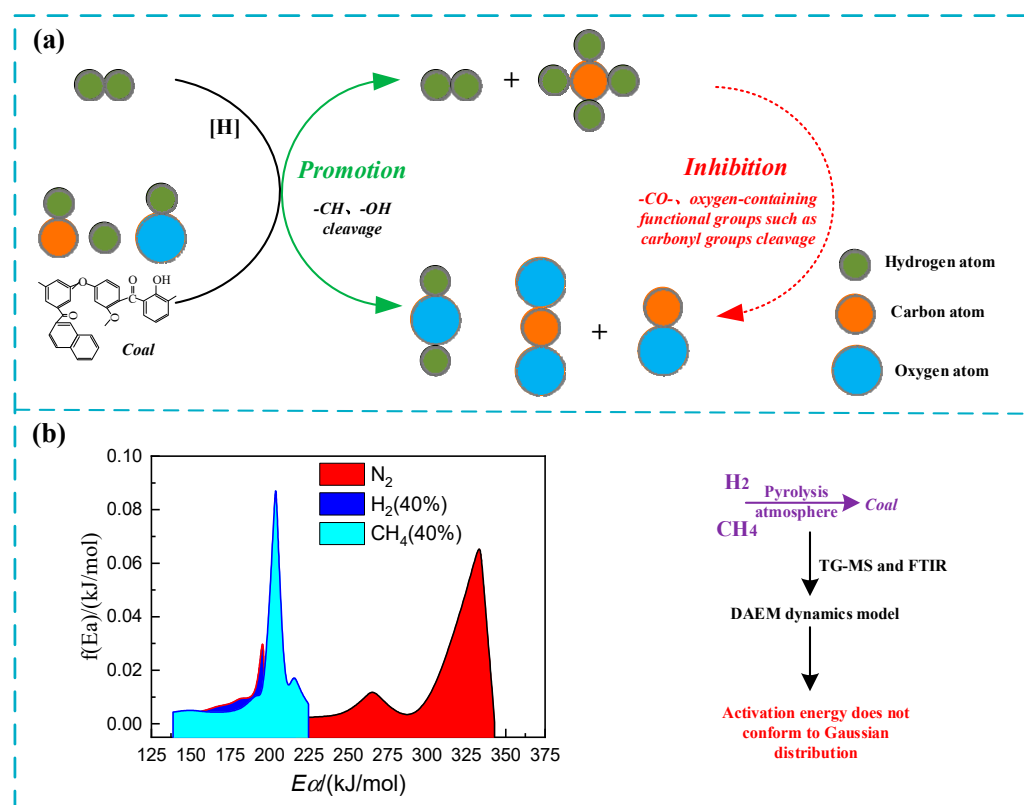


Figure 9. Schematic diagram of the reaction process: (a) The process of H₂ and coal pyrolysis and; (b) The activation energy distribution under the DAEM model.

4. Conclusions

The pyrolysis of raw coal under different atmospheres shows some variability, the activation energy distribution does not satisfy the Gaussian function and has a narrow distribution, and the conversion rate is high in CH₄ atmosphere under the same pyrolysis conditions, thus providing a reference for the pyrolysis of this low-rank coal, specifically including the following conclusions:

- (1) The H₂ (40%) atmosphere obviously promotes the second and third stages of coal pyrolysis weight loss (higher than 380 °C). H₂ promotes the formation of H₂, CH₄, and H₂O by providing the combination of active hydrogen groups with CH groups and –OH functional groups in coal and promoting the cracking of CH functional groups. The H₂ (40%) and CH₄ (40%) atmospheres inhibit the cracking of oxygen-containing functional groups such as carbonyl and C–O groups, and this is not conducive to the formation of CO₂ and CO.
- (2) In the same pyrolysis temperature range, the pyrolysis weight loss rate of raw coal will decrease with the increase of heating rate, and the pyrolysis weight-loss curve

will move to the high-temperature zone. The pyrolysis conversion is in the range of 0.2~0.7, $\ln(\beta/T^2)$ has a good linear correlation with $1/T$, and R^2 is above 0.95. At the same conversion and pyrolysis temperature, the pyrolysis activation energy of the H₂ (40%) and CH₄ (40%) pyrolysis atmospheres is lower than that of the N₂ atmosphere. The activation energy of low-rank coal in N₂, H₂ (40%), and CH₄ (40%) pyrolysis atmospheres does not accord with Gaussian distribution.

- (3) H₂ (40%) and CH₄ (40%) atmospheres promote the release of H₂, CH₄, H₂O, and other products during coal pyrolysis; promote the weight loss of coal pyrolysis; and reduce the activation energy required for coal pyrolysis. The pyrolysis activation energy, E_a , distribution is narrow in the H₂ (40%) atmosphere and CH₄ (40%) atmosphere: the H₂ (40%) atmosphere's E_a is concentrated in the range 17~215 kJ/mol, while the E_a in the CH₄ (40%) atmosphere is concentrated in the range of 225~230 kJ/mol, and the E_a in the H₂ (40%) atmosphere is at the same conversion pyrolysis atmosphere below CH₄ (40%).

Author Contributions: Methodology, H.W.; formal analysis, C.Z. and X.L.; investigation, X.L.; writing—original draft preparation, C.Z. and W.W.; writing—review and editing, M.R. and H.W.; supervision, M.R. and W.W. All authors have read and agreed to the published version of the manuscript.

Funding: The authors gratefully acknowledged the National Natural Science Foundation of China (No.51904223); Young Talents Support Program of the Science and Technology Association of Shaanxi, China (No. 20190603); Shaanxi Province Key R & D General Project-Industrial Field, China (No. 2021GY-128); and Natural Science Basic Research Program of Shaanxi, China (Program No. 2021JQ-505).

Institutional Review Board Statement: Not applicable.

Informed Consent Statement: Not applicable.

Data Availability Statement: The data that support the findings of this study are available from the corresponding author, [Chong Zou], upon reasonable request.

Conflicts of Interest: The authors declare no competing financial interest.

References

- Lin, Y.K.; Li, Q.S.; Li, X.F. Pyrolysates distribution and kinetics of Shenmu long flame coal. *Energy Convers. Manag.* **2014**, *86*, 428–434. [[CrossRef](#)]
- Zou, C.; Ma, C.; Zhao, J.X. Research status and suggestion of mid-low temperature pyrolysis semi-coke as the PCI fuel in blast furnace. *Clean Coal Technol.* **2017**, *23*, 57–64.
- Sun, Q.L.; Li, W.; Chen, H.K. Composition of coal tar from pyrolysis and hydrolysis of Shenmu coal macerals. *J. Fuel Chem. Technol.* **2005**, *33*, 412–415.
- Chen, H.K.; Li, B.Q.; Zhang, B.J. Composition of coal derived tars and its relationship with coal network structure. *J. Fuel Chem. Technol.* **1997**, *25*, 564–565.
- Cai, H.-Y.; Güell, A.; Chatzakis, I.N. Combustion reactivity and morphological change in coal chars: Effect of pyrolysis temperature, heating rate and pressure. *Fuel* **1996**, *75*, 15–24. [[CrossRef](#)]
- Yang, H.P.; Chen, H.P.; Ju, F.D. Influence of pressure on coal pyrolysis and char gasification. *Energy Fuels* **2007**, *21*, 3165–3170. [[CrossRef](#)]
- Wu, H.; Zou, C.; He, J.Y. Effect of low-rank coal pyrolysis conditions on combustion performance and kinetic characteristics of semi-coke for blast furnace injection. *Chin. J. Process. Eng.* **2020**, *20*, 449–457.
- She, Y.; Zou, C.; Liu, S.W. Combustion and gasification characteristics of low-temperature pyrolytic semi-coke prepared through atmosphere rich in CH₄ and H₂. *Green Process. Synth.* **2021**, *10*, 189–200. [[CrossRef](#)]
- Zhang, J.T.; Shi, R.K.; Niu, B. Effect of CH₄ atmosphere on tar yield and quality in coal pyrolysis at low-medium pyrolysis temperature. *J. China Coal Soc.* **2021**, *46*, 292–299.
- Zhong, M.; Ma, F.Y. Analysis of product distribution and quality for continuous pyrolysis of coal in different atmospheres. *J. Fuel Chem. Technol.* **2013**, *41*, 1427–1436.
- Fidalgo, B.; Van Niekerk, D.; Millan, M. The effect of syngas on tar quality and quantity in pyrolysis of a typical South African inertinite-rich coal. *Fuel* **2014**, *134*, 90–96. [[CrossRef](#)]
- Jin, H.; Zhao, X.; Guo, L.J. Experimental investigation on methanation reaction based on coal gasification in supercritical water. *Int. J. Hydrog. Energy* **2017**, *42*, 4636–4641.

13. Sun, Q.L.; Li, W.; Chen, H.K. Comparison Between DAEM and Coats-Redfern Method for Combustion Kinetics Coal Char. *CIESC J.* **2003**, *54*, 1598–1602.
14. Qin, L.N.; Li, L.J.; Zhou, A.L. Establishment of dynamics model for coal pyrolysis. *Clean Coal Technol.* **2014**, *134*, 92–96.
15. Ulloa, C.; Gordon, A.L.; García, X. Distribution of activation energy model applied to the rapid pyrolysis of coal blends. *J. Anal. Appl. Pyrolysis* **2004**, *71*, 465–483. [[CrossRef](#)]
16. Wu, H.; Zheng, J.F.; Zou, C. Numerical analysis of kinetics of char combustion process and selection of mechanism functions. *J. Therm. Anal. Calorim.* **2021**, *147*, 3217–3227. [[CrossRef](#)]
17. Vand, V. A theory of the irreversible electrical resistance changes of metallic films evaporated in vacuum. *Proc. Phys. Soc. London* **1943**, *55*, 222. [[CrossRef](#)]
18. Pitt, G.; Millward, G.R. Coal and modern coal processing: An introduction. *Chem. Eng. Edu.* **1979**, *15*, 186–219.
19. Miura, K. A new and simple method to estimate $f(E)$ and $k_0(E)$ in the distributed activation energy model from three sets of experimental data. *Energy Fuels* **1995**, *9*, 302–307. [[CrossRef](#)]
20. Heidenreich, C.A.; Yan, H.; Zhang, D. Mathematical modelling of pyrolysis of large coal particles—Estimation of kinetic parameters for methane evolution. *Fuel* **1999**, *78*, 557–566. [[CrossRef](#)]
21. Alonso, M.; Alvarez, D.; Borrego, A. Systematic effects of coal rank and type on the kinetics of coal pyrolysis. *Energy Fuels* **2001**, *15*, 413–428. [[CrossRef](#)]
22. Zhang, K.; You, C.F. Research on the Parallel Reaction Kinetic Model of Lignite Pyrolysis. *Proc. China Soc. Electr. Eng.* **2020**, *31*, 26–31.
23. Li, C.J.; Jiang, H.; Zhao, J.M. Lignite Pyrolysis Characteristics of Thermogravimetric Analysis and DAEM Model Analysis. *Energy Conserv. Technol.* **2015**, *33*, 69–71.
24. Zhao, Y.M.; Qiu, P.H.; Xie, X. Analysis on applicability of distributed activation energy model in coal pyrolysis kinetics. *Coal Conv.* **2017**, *40*, 13–18.
25. Wang, F.; Zeng, X.; Wang, Y.G. Investigation on in/ex-situ coal char gasification kinetics in a micro fluidized bed reactor. *J. Fuel Chem. Technol.* **2015**, *43*, 393–401.
26. Miura, K.; Maki, T. A Simple Method for Estimating $f(E)$ and $k_0(E)$ in the Distributed Activation Energy Model. *Energy Fuels* **1998**, *12*, 864–869. [[CrossRef](#)]
27. Yu, J.; Zhang, M.C. A Simple Method for Predicting the Rate Constant of Pulverized-coal Pyrolysis at Higher Heating Rate. *Energy Fuels* **2003**, *133*, 107–117. [[CrossRef](#)]
28. Li, Q.Z.; Lin, B.Q.; Zhao, C.S. Chemical structure analysis of coal semi-coke surface based on Fourier-transform infrared spectrometer. *Proce CSEE.* **2011**, *31*, 46–52.
29. Burnham, A.K.; Braun, R.L. Global Kinetic Analysis of Complex Materials. *Energy Fuels* **1999**, *13*, 1–22. [[CrossRef](#)]
30. Wang, J.L.; Li, P.; Liang, L.T. Kinetics modeling of low-rank coal pyrolysis based on a three-Gaussian distributed activation energy model (DAEM) reaction model. *Energy Fuels* **2016**, *30*, 9693–9702. [[CrossRef](#)]
31. Zhang, S.F.; Zhu, F.; Bai, C.G. Thermal behavior and kinetics of the pyrolysis of the coal used in the COREX process. *J. Anal. Appl. Pyrolysis* **2013**, *104*, 660–666. [[CrossRef](#)]
32. Guizani, C.; Sanz, F.E.; Salvador, S. Effects of CO₂ on biomass fast pyrolysis: Reaction rate, gas yields and char reactive properties. *Fuel* **2014**, *116*, 310–320. [[CrossRef](#)]
33. De Jong, W.; Di Nola, G.; Venneker, B. TG-FTIR pyrolysis of coal and secondary biomass fuels: Determination of pyrolysis kinetic parameters for main species and NOx precursors. *Fuel* **2007**, *86*, 2367–2376. [[CrossRef](#)]
34. Arenillas, A.; Pevida, C.; Rubiera, F. Characterisation of model compounds and a synthetic coal by TG/MS/FTIR to represent the pyrolysis behaviour of coal. *J. Anal. Appl. Pyrolysis* **2004**, *71*, 747–763. [[CrossRef](#)]
35. Chen, X.Y.; Liu, L.; Zhang, L.Y. Pyrolysis characteristics and kinetics of coal-biomass blends during co-pyrolysis. *Energy Fuels* **2019**, *33*, 1267–1278. [[CrossRef](#)]
36. Sun, Q.L.; Li, W.; Chen, H.K. The variation of structural characteristics of macerals during pyrolysis ☆. *Fuel* **2003**, *82*, 669–676. [[CrossRef](#)]
37. Liu, L.L.; Kumar, S.; Wang, Z.H. Catalytic effect of metal chlorides on coal pyrolysis and gasification part I. Combined TG-FTIR study for coal pyrolysis. *Thermochim. Acta* **2017**, *655*, 331–336. [[CrossRef](#)]
38. Niu, Z.Y.; Liu, G.J.; Yin, H. Effect of pyridine extraction on the pyrolysis of a perhydrous coal based on in-situ FTIR analysis. *J. Energy Inst.* **2019**, *92*, 428–437. [[CrossRef](#)]
39. Please, C.P.; McGuinness, M.J.; McElwain, D.L.S. Approximations to the distributed activation energy model for the pyrolysis of coal. *Combust. Flame* **2003**, *133*, 107–117. [[CrossRef](#)]

Disclaimer/Publisher's Note: The statements, opinions and data contained in all publications are solely those of the individual author(s) and contributor(s) and not of MDPI and/or the editor(s). MDPI and/or the editor(s) disclaim responsibility for any injury to people or property resulting from any ideas, methods, instructions or products referred to in the content.